Electronic Structure and Light-Induced Conductivity of a Transparent Refractory Oxide

J. E. Medvedeva,[1] A. J. Freeman,[1] M. I. Bertoni,[2] and T. O. Mason[2]
[1]*Department of Physics and Astronomy, Northwestern University, Evanston, Illinois 60208-3112, USA*
[2]*Department of Materials Science and Engineering, Northwestern University, Evanston, Illinois 60208-3112, USA*
(Received 12 November 2003; published 1 July 2004)

Combined first-principles and experimental investigations reveal the underlying mechanism responsible for a drastic change of the conductivity (by 10 orders of magnitude) following hydrogen annealing and UV irradiation in a transparent oxide, $12CaO \cdot 7Al_2O_3$, found by Hayashi *et al.* [Nature (London) **419**, 462 (2002).] The charge transport associated with photoexcitation of an electron from H^- occurs by electron hopping. We identify the atoms participating in the hops, determine the exact paths for the carrier migration, estimate the temperature behavior of the hopping transport, and predict a way to enhance the conductivity by specific doping.

DOI: 10.1103/PhysRevLett.93.016408 PACS numbers: 71.20.–b, 72.20.Ee, 72.40.+w, 81.05.Je

The rare combination of transparency and conductivity has a wide range of technological applications [1]. Until recently, optimum optical transmission and useful electrical conductivity ($> 10^3$ S cm^{-1}) was attained by the introduction of selected dopants into a wide-band-gap oxide. Hence the excitement surrounding the report that Hayashi *et al.* found a new way to convert a transparent oxide into a persistent electronic conductor [2] with the potential for less expensive and more flexible optoelectronic devices. Despite careful experimental studies, no definitive understanding has been reached on the underlying mechanism responsible for this new dramatic effect. In this combined theoretical and experimental investigation, we address the nature of this novel phenomenon which is crucial for further progress and make predictions on how to improve the conductivity toward the level where it becomes useful for practical applications.

We have reproduced in bulk form the single crystal and thin film results of Hayashi *et al.* by solid state reaction of high purity oxides [3] (99.99 + %), followed by hydrogen treatment ($5\%H_2/95\%N_2$) of sintered pellets at 1300 °C for 2 h, and by quenching to room temperature. UV treatment was performed under a mercury arc lamp (40 min at 20 mW cm^{-2} and a wavelength of 220 nm). This turned a surface layer of $\sim$16 μm thickness from white to green, with a conductivity changed from 10^{-10} to 0.6 S cm^{-1} (by the four-point method). We also irradiated loose H-treated powders, which also turned from white to a uniform green color, and measured their conductivity by a "powder-solution-composite" method [4] to be 0.41 S cm^{-1}. Both values agree with those in Ref. [2] and provide confidence in our experimental confirmation of the predictions reported below.

From the theoretical side, we demonstrate with density functional calculations that the conductivity appears to result from electrons excited off the H^- ions into conduction bands formed from Ca 3*d* states. The changes found in the electronic properties caused by the UV irradiation of H-doped mayenite allow us to conclude that the observed absorption peak at 0.4 eV has a fundamentally different nature than the F^+ center energy level originally assumed in Ref. [2] and followed in recent theoretical work [5]. Our calculated charge density shows clearly that electron trapping on a vacancy (i.e., formation of the F^+ center) does not occur [6]. Instead, we identify the atoms participating in hopping transport; estimates of the temperature behavior of the conductivity agree reasonably well with experiment. Finally, we found a strong dependence of the electronic transport on the particular hopping centers and their spatial arrangement that allows the prediction of rates of temperature treatment and dopants which will enhance the conductivity.

The crystal structure of $12CaO \cdot 7Al_2O_3$ has the space group $I\bar{4}3d$, with 2 f.u. in the unit cell and a lattice parameter of 11.98 Å [7,8]. This framework includes 64 of the oxygen atoms; the remaining two oxygen ions which provide charge neutrality [8] are located inside the cages; see Fig. 1(a). These two O^* are distributed between 24 sites that produce a structural disorder. From full-potential linearized augmented plane-wave [9] total energy calculations of seven structures with different distances between these two oxygen ions (ranging from 5.1 to 10.4 Å), we found that the O^*s tend to maximize the distance between them by forming a bcc lattice with the crystallographic basis oriented randomly with respect to that of the whole crystal. After H annealing, changes in the crystal structure are not observed [10]. The incorporation of H corresponds to the chemical reaction [11]: $O^{2-}(\text{cage}) + H_2(\text{atm.}) \rightarrow OH^-(\text{cage}) + H^-(\text{another cage})$, so the unit cell contains two cages occupied by O^*H^-, another two by H^- (abbreviated as H^*), and the remaining eight cages are empty [12].

The calculated [13] electronic density of states (DOS) before H doping is shown in Fig. 1(b): oxygen 2*p* states form the top of the valence band between -6 and -2 eV (the Fermi level is taken as zero), while the bottom of the conduction band is formed from Ca 3*d* states. Located

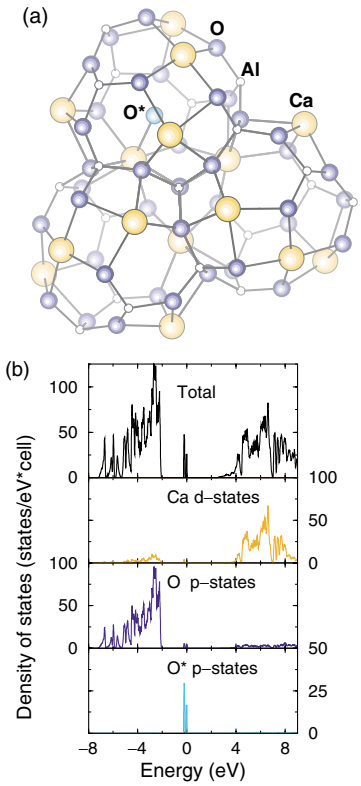

FIG. 1 (color online). (a) Three of the 12 cages constituting a unit cell of mayenite. An O^{2-} anion (abbreviated as O^*) is located inside one of six cages so that the distances between O^* and its six neighbor Ca atoms vary from 2.36 to 3.95 Å. (b) Total and partial DOS of $12CaO \cdot 7Al_2O_3$; E_F is at 0 eV. The Al $3d$ states form the band centered at ~28 eV.

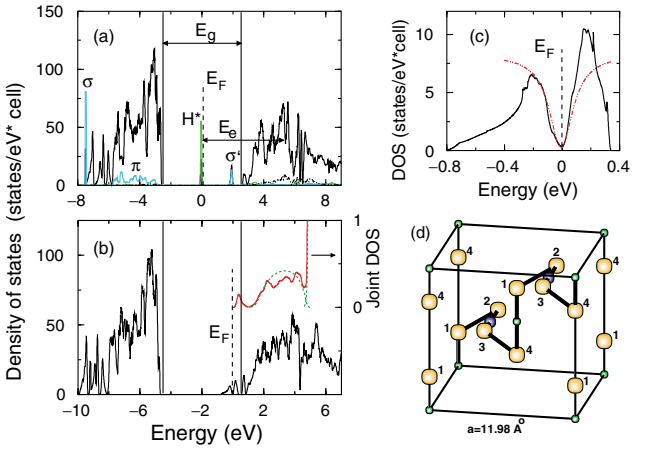

FIG. 2 (color online). (a) Total DOS of H-doped mayenite. The band gap, E_g, is between O $2p$ and Ca $3d$ states. The DOS of the OH^- and H^* bands is enlarged by a factor of 5. The UV activation corresponds to the transition from H^* $1s$ states to the $3d$ states of its closest Ca (dashed line), with energy E_e. (b) Total DOS of UV-irradiated H-doped mayenite and the joint DOS calculated using the optical selection rules and only nearest neighbor transitions which have higher probability; the dashed line is a guide to the eyes. (c) Enlarged total DOS of UV-irradiated H-doped mayenite and a theoretical fit (dashed line); see the text. (d) The optimal path for electron migration. The cube represents a full unit cell consisting of 12 cages (118 atoms); only atoms which give the dominant contribution to $g(E_F)$ are shown—Ca (largest spheres), O^* [between Ca(2) and Ca(3)], and H^* (smallest spheres).

inside one of the six cages, O^* gives a fully occupied impurity peak below E_F. The calculated band gap, 4.8 eV, underestimates the experimental absorption edge [2] by 4%. The incorporation of hydrogen results in the appearance of new bands, Fig. 2(a): (i) since H shares its electron with O^* (and forms an OH^- complex), filled σ and nonbonding π bands and unoccupied σ' band are introduced; (ii) the $1s$ states of H^* form the fully occupied impurity band below E_F. After the H doping, the energy of the transitions from O $2p$ states to Ca $3d$ states is decreased by 0.7 eV (from 5.9 to 5.2 eV), in agreement with experiment [2]. The maximum efficiency of the UV activation of the H^*, which corresponds to transitions from H^* $1s$ states to the $3d$ states of its closest Ca neighbors, occurs at about the same photon energy, Fig. 2(a). These results are in contrast with the conclusion of Ref. [2] that hydrogen controls the absorption edge.

For UV-irradiated H-bearing mayenite, we calculated the model system where the electron released from H^* ($H^- \rightarrow H^0 + e^-$) is transferred equally to the d states of six Ca neighbors [15]. The self-consistent DOS shows the formation of a new band [Fig. 2(b)] with the same total number of states, m, as in the band gap of the system before UV irradiation. However, since m is now 2 times larger than the number of available electrons, E_F passes through the middle of the band and the system becomes conducting. The calculated positions of the characteristic absorption bands [0.38 and 3.5 eV, Fig. 2(b)] agree with experiment (0.4 and 2.8 eV), as is the intense charge transfer transition from oxygen $2p$ states to Ca $3d$ states which occurs at ~4.8 eV.

The nonzero DOS at E_F, $g(E_F)$, is found to be determined mainly by H^*, O^*, and Ca states—atoms that are spatially well separated from each other [Fig. 2(d)], which points to the hopping nature of the conductivity [16]. It is striking that the arrangement of the atoms corresponds to the shortest electron hopping path: only the closest Ca neighbors of O^*, Ca(2) and Ca(3) (at distances of 3.3 and 2.4 Å, respectively), and the closest Ca neighbors of H^*, Ca(1) and Ca(4) (both at 2.8 Å), give significant contributions to $g(E_F)$ (Table I). The longest segment on the hopping path corresponds to the distance between Ca(1), Ca(2), and O^*, which explains the higher probability to find the electron on Ca(1) and Ca(2). Finally, the charge density distribution calculated in the energy window of 25 meV below E_F clearly shows the connected electron density maxima along the hopping path [cf. Fig. 3(a)]. The charge density in the empty cages is insignificant [cf. Fig. 3(b)], demonstrating that trapping of the electron on the vacancy does not occur.

Hopping transport in systems with localized electronic states has been studied analytically, numerically, and

TABLE I. The relative contributions per atom to the DOS at E_F. Similar percentages are obtained from the integrated DOS in the energy range of $E_F \pm 0.025$ eV.

Atoms	%	Atoms	%	Atoms	%
Ca(1)	7.6	Ca(4)	4.2	rest Ca	~1.0
Ca(2)	8.4	H*	6.9	rest O	~0.7
O*	8.3	Centers of		Al	0.1
Ca(3)	3.8	empty cages	0.3		

experimentally [17–19]. At high temperatures (T) the hopping occurs between nearest neighbors and has an activated nature. At lower T, the activation energy for hops between localized centers can be reduced by enlarging the hopping distance—which leads to the variable-range hopping described by Mott and Davis [17]. At yet lower T, the electron-electron repulsive interaction between charge carriers may result in the formation of a Coulomb gap [18] centered at E_F. The value of the gap can be estimated as $e^2/4\pi\varepsilon_0\varepsilon r_{\rm ch}$, where e is the elementary charge, ε_0 is the permittivity constant, ε is the relative dielectric constant, and $r_{\rm ch}$ is the characteristic distance between interacting electrons. In the present case, $r_{\rm ch}$ is equal to the cube root of the unit cell volume divided by 2. Using [20] $\varepsilon = 2.56$ yields 0.3 eV for the gap value which agrees with the observed [2] absorption peak at 0.4 eV.

Similar to the above qualitative picture, we predict the behavior of the conductivity at finite T based on the calculated DOS in the vicinity of E_F for irradiated H-doped mayenite. Clearly, this exhibits in Fig. 2(c) a soft [21] Coulomb gap near E_F and, similar to Fig. 10.1 in Ref. [18], has two peaks. Moreover, the splitting of the hybrid band, 0.38 eV, agrees well with the value of the gap estimated above on the basis of the strong electron repulsion. These results indicate the Efros-Shklovskii (ES) behavior [18] of the conductivity σ at low T: $\sigma = \sigma_0 \exp[-(T_{\rm ES}/T)^{1/2}]$ with $T_{\rm ES} = \beta_{\rm ES} e^2/k_B k\xi$, where ξ is the localization length, k_B is the Boltzmann constant, and $k = \varepsilon_0\varepsilon$. When T increases, the Coulomb gap fills. A substantial DOS should be observed already at $T \sim 0.05\Delta\epsilon$, where $\Delta\epsilon$ is the gap width [22]. At this T, the changeover to the Mott behavior [17] should occur: $\sigma = \sigma_0 \exp[-(T_M/T)^{1/4}]$, with $T_M = \beta_M/k_B g_0 \xi^3$. The double peak structure completely disappears at $T \sim 0.4\Delta\epsilon$. Using $\Delta\epsilon \simeq 0.38$ eV [Fig. 2(c)], we obtain the crossover T between Mott and ES behavior to be $T_c \simeq 220$ K. Indeed, for H-doped UV-irradiated mayenite, the $T^{-1/4}$ dependence of $\log(\sigma)$ was found experimentally [2] for $50 < T < 300$ K.

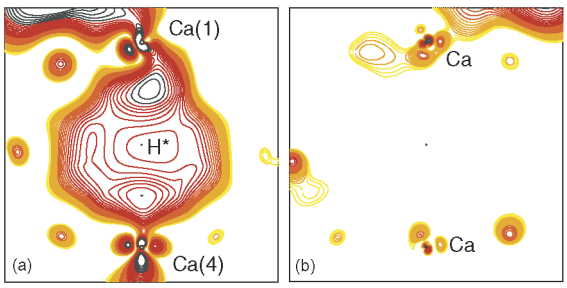

FIG. 3 (color online). Contour map of the charge density distribution within a slice passing through the center of (a) a cage with H* and (b) an empty one (vacancy).

The calculated DOS near E_F fits well [Fig. 2(c)] with the theoretical one of the form $g(E) = \alpha E_c^2 E^2/(E_c^2 + E^2)$, where $\alpha = (3/\pi)(k^3/e^6)$. In the high energy limit, the DOS has the constant value of $g_0 \equiv \alpha E_c^2$ that corresponds to Mott behavior. In the opposite limit, it approaches a parabolic dependence (ES) which has only one physical parameter—the refractive index, n. We found $n \simeq 2.1$, while the experiment [20] gives $n = 1.6$. From the fit, we obtain $g_0 \simeq 8$ states/eV · cell and $\alpha \simeq 800$ which allows us to estimate the characteristic T: using $\beta_M = 7.6$ [23], $\beta_{\rm ES} = 2.8$ [18], and the localization length $\xi = 1.5$ Å (which is comparable to the ionic radii of the atoms involved in the hops), we obtain $T_M \simeq 5.6 \times 10^6$ K, which agrees fairly well with the experimental value [2], $T_M = 2 \times 10^6$ K, and we predict that $T_{\rm ES} \simeq 2.7 \times 10^4$ K.

Since H* may also occupy cages located farther away from the one with an OH^-, we investigated this arrangement and found it to be less favorable energetically—by 96 meV. However, under the rapid cooling of the sample annealed at 1300 °C some H* can become "frozen" into these positions. After UV irradiation, the corresponding hopping path involves a long segment between two Ca atoms (now increased from 3.7 to 6.5 Å), so that $g(E_F)$ becomes zero and the hopping has an activated behavior. If now T is increased to a level sufficient for hydrogen migration, these H* will be able to diffuse into the energetically favorable positions which facilitates the hopping and leads to an increase of σ. We confirmed these predictions experimentally, as shown in Fig. 4. Moreover, nonreversible behavior is seen for $T > T_m$, the conductivity maximum: the decay of σ is associated with recombination $H^0 + e^- \rightarrow H^-$ and H_2 release which breaks up the hopping path.

The strong dependence of the conductivity on the particular atoms participating in the hopping suggests the possibility of varying the conductivity by proper doping. For example, we expect that Mg substitution can lead to a decrease in σ once Mg substitutes one of the Ca atoms involved in the hopping, since its $3d$ states will lie much higher in energy than that of Ca, while Sr substitution may not result in any significant changes in σ. Instead, one way to possibly improve the electronic transport consists in increasing the concentration of hopping centers. For this, the encaged poorly bonded O^{2-} ion is easily replaced by $2F^-$ or $2Cl^-$ ions that will allow an enhancement of σ since the number of hopping centers and the number of carriers is now doubled. Recent observations on proton implantation [24] agree with our model and its predictions: our calculations show that along with the

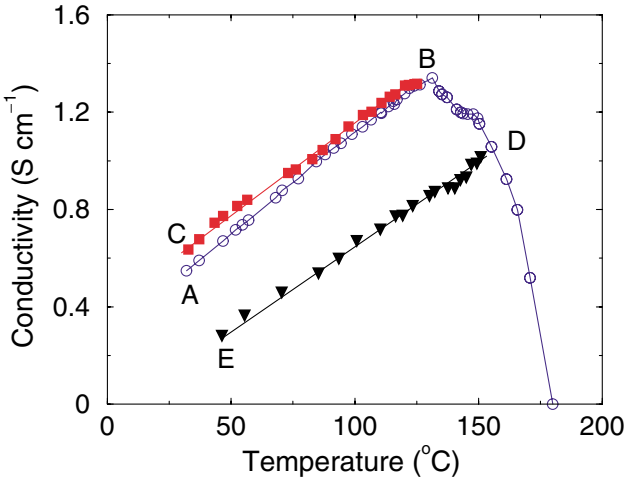

FIG. 4 (color online). Measured σ-T characteristics of the UV-irradiated H-doped $12CaO \cdot 7Al_2O_3$ bulk samples of 46% density. Because of the realization of the optimal arrangement of the hopping centers during the heat treatment ($A \rightarrow B$), σ is enhanced after cooling the sample ($B \rightarrow C$). Subsequent T cycling ($B \leftrightarrow C$) does not result in any changes of σ,; i.e., the system is reversible. Cooling from any point above the conductivity maximum, as in path ($D \rightarrow E$), shows reduced σ unchanged by UV irradiation ($E \leftrightarrow D$), as expected from the release of H.

increased concentration of the "excess" electrons, the proton implantation will result in the appearance of new unoccupied states in the band gap making H^+ one of the hopping centers that creates a conductivity channel and so enhances the transport.

Finally, the encouraging findings obtained in this first *ab initio* study of hopping transport suggest that important results may also be obtained when a similar approach is applied to such systems as doped semiconductors, manganite perovskites, carbon nanotubes, etc. [25].

We thank V. P. Dravid for sharing his unpublished electron microscopy results. Work supported by the DOE (Grant No. DE-FG02-88ER45372) and by the NSF through its MRSEC program at the Northwestern Materials Research Center. Computational resources have been provided by the DOE supported NERSC.

[1] G. Thomas, Nature (London) **398**, 907 (1997); D. S. Ginley and C. Bright, MRS Bull. **25**, 15 (2000), and references therein.
[2] K. Hayashi, S. Matsuishi, T. Kamiya, M. Hirano, and H. Hosono, Nature (London) **419**, 462 (2002).
[3] H. Hosono and Y. Abe, Inorg. Chem. **26**, 1192 (1987).
[4] B. J. Ingram and T. O. Mason, J. Electrochem. Soc. **150**, E396 (2003).
[5] P. V. Sushko, A. L. Shluger, K. Hayashi, M. Hirano, and H. Hosono, Phys. Rev. Lett. **91**, 126401 (2003); P.V. Sushko, A. L. Shluger, K. Hayashi, M. Hirano, and H. Hosono, Thin Solid Films **445**, 161 (2003).
[6] That mayenite falls into the fit of Fig. 4(b) in Ref. [2] and, hence, into the F^+ center category, appears fortuitous. Our *ab initio* investigations show that the absorption band energy of the F^+ center in relaxed CaO depends strongly on tetragonal distortions: for the *same average* cation-anion distance, a tetragonal distortion of 1% (and 2%) results in an energy deviation of 2% (and 6%). In mayenite, the distortion is 25%; therefore, the energy deviation will be much larger. Thus, the use of an *average* cation-anion distance for mayenite [2] in the Mollwo-Ivey law is incorrect.
[7] H. Bartl and T. Scheller, Neues Jahrb. Mineral., Monatsh. **35**, 547 (1970); A. N. Christensen, Acta Chem. Scand. A **41**, 110 (1987).
[8] J. A. Imlach, L. S. D. Glasser, and F. P. Glasser, Cem. Concr. Res. **1**, 57 (1971).
[9] E. Wimmer, H. Krakauer, M. Weinert, and A. J. Freeman, Phys. Rev. B **24**, 864 (1981).
[10] V. P. Dravid (unpublished)
[11] The structure with two H^- ions in cages and released O_2 gas [2] leads to an insulating state after UV activation.
[12] The positions of the H ions were optimized using the DMol method; see B. Delley, J. Chem. Phys. **113**, 7756 (2000).
[13] We employ the linear muffin-tin orbital method in the atomic sphere approximation [14] for the cell of $12CaO \cdot 7Al_2O_3$ with 1 f.u., i.e., a total of 59 atoms per cell which combine into six cages; 85 empty spheres were included to fill out the open space.
[14] O. K. Andersen, O. Jepsen, and M. Sob, *Electronic Band Structure and its Applications,*, edited by M. Yussouff (Springer-Verlag, Berlin, 1986).
[15] We used the virtual crystal approximation which accounts properly for the band-filling effects.
[16] We found that after UV irradiation, the H^* is displaced from its original symmetric position which explains the observed persistence of the conducting state.
[17] N. F. Mott and E. A. Davis, *Electronic Processes in Noncrystalline Materials* (Oxford University Press, Oxford, 1979).
[18] B. I. Shklovskii and A. L. Efros, *Electronic Properties of Doped Semiconductors* (Springer-Verlag, Berlin, Heidelberg, 1984).
[19] H. Böttger and V.V. Bryksin, *Hopping Conduction in Solids* (Akademie-Verlag, Berlin, 1985); N. Van Lien and R. Rosenbaum, J. Phys. Condens. Matter **10**, 6083 (1998); A. G. Zabrodskii, Philos. Mag. B **81**, 1131 (2001).
[20] G. I. Zhmoidin and G. S. Smirnov, Inorg. Mater. **18**, 1595 (1982).
[21] The residual $g(E_F)$ may be caused by correlated simultaneous hops of several electrons (multielectron hopping) which play a dominant role at extremely low T; see M. Pollak and M. L. Knotek, J. Non-Cryst. Solids **32**, 141 (1979).
[22] M. Sarvestani, M. Schreiber, and T. Vojta, Phys. Rev. B **52**, R3820 (1995).
[23] N. F. Mott, *Conduction in Non-Crystalline Materials* (Clarendon Press, Oxford, 1987), p. 28.
[24] M. Miyakawa, K. Hayashi, M. Hirano, Y. Toda, T. Kamiya, and H. Hosono, Adv. Mater. **15**, 1100 (2003).
[25] M. Pollak, Phys. Status Solidi (b) **230**, 295 (2002).